Roles of Active Site Aromatic Residues in Catalysis by Ketosteroid Isomerase from *Pseudomonas putida* Biotype B†

Do-Hyung Kim, Gyu Hyun Nam, Do Soo Jang, Gildon Choi, Soyoung Joo, Jeong-Sun Kim, Byung-Ha Oh, and Kwan Yong Choi*

Department of Life Sciences and Center for Biofunctional Molecules, Pohang University of Science and Technology, Pohang 790-784, South Korea

Received May 6, 1999; Revised Manuscript Received July 22, 1999

ABSTRACT: The aromatic residues Phe-54, Phe-82, and Trp-116 in the hydrophobic substrate-binding pocket of Δ^5-3-ketosteroid isomerase from *Pseudomonas putida* biotype B have been characterized in their roles in steroid binding and catalysis. Kinetic and equilibrium binding analyses were carried out for the mutant enzymes with the substitutions Phe-54 → Ala or Leu, Phe-82 → Ala or Leu, and Trp-116 → Ala, Phe, or Tyr. The removal of their bulky, aromatic side chains at any of these three positions results in reduced k_{cat}, particularly when Phe-82 or Trp-116 is replaced by Ala. The results are consistent with the binding interactions of the aromatic residues with the bound steroid contributing to catalysis. All the mutations except the F82A mutation increase K_m; the F82A mutation decreases K_m by ca. 3-fold, suggesting a possibility that the phenyl ring at position 82 might be unfavorable for substrate binding. The K_D values for *d*-equilenin, an intermediate analogue, suggest that a space-filling hydrophobic side chain at position 54, a phenyl ring at position 82, and a nonpolar aromatic or small side chain at position 116 might be favorable for binding the reaction intermediate. In contrast to the increased K_D for equilenin, the enzymes with any substitutions at positions 54 and 116 display a decreased K_D for 19-nortestosterone, a product analogue, indicating that Phe-54 and Trp-116 might be unfavorable for product binding. The crystal structure of F82A determined to 2.1-Å resolution reveals that Phe-82 is important for maintaining the active site geometry. Taken together, our results demonstrate that Phe-54, Phe-82, and Trp-116 contribute differentially to the stabilization of steroid species including substrate, intermediate, and product.

Δ^5-3-Ketosteroid isomerase (KSI)[1] is an enzyme catalyzing the allylic isomerization of a variety of Δ^5-3-ketosteroids to Δ^4-3-ketosteroids by an intramolecular transfer of the 4β-proton to the 6β-position via an enolate intermediate (Scheme 1) (*1*−*4*). It has been under intensive investigations as a prototype for elucidating the enzyme mechanism of the allylic rearrangement (*5*−*9*). KSI is one of the most proficient enzymes exhibiting a high second-order rate constant of k_{cat}/K_m comparable to the kinetic rate of a diffusion-controlled reaction (*10*).

Despite what is known about KSI, fundamental controversies remain regarding the origin of its intermediate stabilization and extremely high enzymatic reaction rate. The structural determination of the enzymes from *Pseudomonas putida* biotype B and *Commamonas testosteroni* (formerly known as *Pseudomonas testosteroni*) by recent X-ray crystallography (*11*, *12*) and NMR spectroscopy (*13*, *14*) has provided insight into the solution of the controversial issues concerning the KSI catalytic mechanism. *P. putida* KSI (PI) and *C. testosteroni* KSI (TI) share a conserved tertiary fold. The structures clearly show that Tyr-14 and Asp-38 (the residues are numbered according to those of TI throughout the text) play a crucial role in enzyme catalysis (*7*, *15*, *16*). Asp-99 has also been found to be involved in a hydrogen bond either with O3 of *d*-equilenin, an intermediate analogue (*11*, *13*), or with Tyr-14 (*14*) contributing to the stabilization of the intermediate. To explain the origin of the extremely high catalytic power, a low-barrier hydrogen bond was proposed to be present between Tyr-14 Oη and O3 of the enolate intermediate (*11*, *12*, *17*, *18*) or between Asp-99 Oδ2 and Tyr-14 Oη (*14*, *19*, *20*).

In addition to these conserved residues, one of the aromatic residues in the active site of TI, Phe-101, has been identified as important for catalysis, leading to the conclusion that the phenyl ring of Phe-101 plays a role in stabilizing the transition state(s) and the intermediate (*21*, *22*). This suggests a possibility that other aromatic residues in the active site of KSI might also play important roles in catalysis. The crystal structure of PI in complex with *d*-equilenin has shown how the ring moieties of the steroid interact with active site

† This research was supported by grants from the Korea Science and Engineering Foundation, the Academic Research Fund of Korea's Ministry of Education, and POSTECH Research Funds and, in part, by the Research Center for New Biomaterials in Agriculture, Seoul National University in Korea.

* To whom correspondence should be addressed. Tel: 82-562-279-2295. Fax: 82-562-279-2199. E-mail: kchoi@postech.ac.kr.

[1] Abbreviations: KSI, ketosteroid isomerase; PI, KSI of *Pseudomonas putida* biotype B; TI, KSI of *Commamonas testosteroni*; 5-AND, 5-androstene-3,17-dione; 5,10-EST, 5,10-estrene-3,17-dione; 4-AND, 4-androstene-3,17-dione; K_D, dissociation constant; *d*-equilenin, *d*-1,3,-5(10),6,8-estrapentaen-3-ol-17-one; 19-nortestosterone, 17β-hydroxy-4-estren-3-one; SDS−PAGE, sodium dodecyl sulfate−polyacrylamide gel electrophoresis; WT, wild-type KSI from *P. putida*; Tris-HCl, tris-(hydroxymethyl)aminomethane hydrochloride; EDTA, ethylenediaminetetraacetic acid; kDa, kilodalton; λ_{max}, the wavelength at which the spectral intensity is highest.

10.1021/bi991040m CCC: $18.00
Published on Web 09/29/1999

Scheme 1

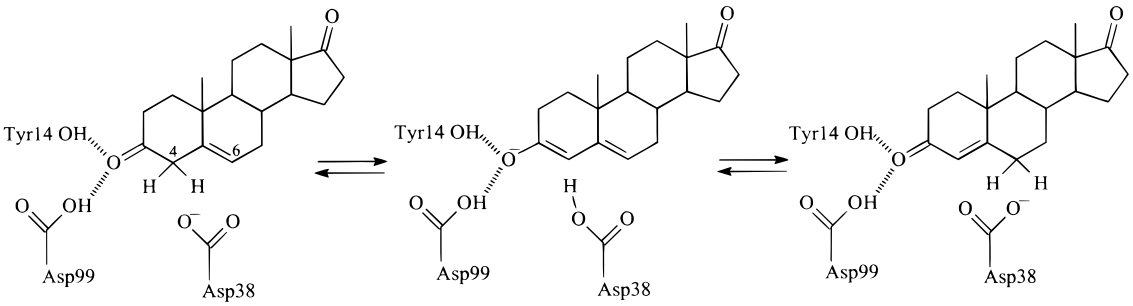

residues (*11*). Most of the active site cleft of PI is lined with such hydrophobic amino acids as Val-18, Ile-26, Phe-52, Leu-59, Val-63, Phe-82, Val-84, Met-86, Leu-95, Met-112, and Trp-116 in addition to the catalytic residues Tyr-14, Asp-38, and Asp-99. Some aromatic residues are noticeably located closely to the steroid (Figure 1). The side chains of Phe-54 and Phe-82 conserved in both PI and TI are located antarafacially to each other with respect to the bound steroid, and their aromatic side chains are oriented to be almost perpendicular to the bound steroid ring system. Phe-54 and Phe-82 lie on the α-helix A3 and the β-strand B4, respectively. The indole ring of Trp-116 lying on β-strand B6 is also located adjacent to the steroid 4−7 Å away. This position is occupied by phenylalanine in TI, suggesting that an aromatic or a bulky hydrophobic group might be necessary at this position. The conservative positioning of the aromatic residues toward the steroid implies that their interactions with the steroid might play an important role in catalysis by KSI.

To understand the roles of active site aromatic residues in catalysis by PI, the interactions mediated by the residues Phe-54, Phe-82, and Trp-116 for binding steroids were perturbed by site-directed mutagenesis. The mutational effects were then analyzed in terms of catalysis and binding affinity toward *d*-equilenin, an intermediate analogue, and 19-nortestosterone, a product analogue. The mutations exhibited differential effects on both kinetic parameters and binding affinities toward the steroid species, which is consistent with the aromatic residues playing differential roles in binding the respective steroid species. The crystal structure of F82A, as determined at 2.1 Å resolution, provides the structural basis for understanding the roles of Phe-82 in interacting with a bound steroid. Our studies show insight into the roles of these aromatic residues in catalysis contributing differentially to the stabilization of substrate, intermediate, and product.

EXPERIMENTAL PROCEDURES

Materials. Chemicals for buffer solutions, deoxycholate, and 19-nortestosterone were purchased from Sigma. Oligonucleotides were obtained from Bioneer Inc. T4 DNA ligase, *Eco*RI, *Ksp*I, *Eco*R47III, *Afl*III, *Spl*I, *Tth*lllII, and *Hin*dIII were supplied by Promega. Equilenin, 5-androstene-3,17-dione (5-AND), and 5,10-estrene-3,17-dione (5,10-EST) were purchased from Steraloids. The Superose 12 gel filtration column and radiochemicals for the nucleotide sequencing were obtained from Amersham Pharmacia Biotech.

Site-Directed Mutagenesis. Phe-54 and Phe-82 were changed to Ala or Leu to make F54A, F54L, F82A, and F82L while Trp-116 was changed to Ala, Phe, and Tyr to make W116A, W116F, and W116Y according to the procedure described previously (*23*). Single-stranded uracil-containing template DNA complementary to the coding strand of the isomerase gene was obtained from the pSW2 (*24*), a pBluescript SK(−) plasmid containing the entire *P. putida* isomerase gene, which had been introduced in *Escherichia coli* RZ1032 after infection with the helper phage M13K07 (Pharmacia). Oligonucleotides of 5′-GAG CAG ATT GCC GCG GCC TAT CGC CAG GGT TT-3′ (F54A), 5′-CCG CGA GCA GAT TGC AGC GCT CTA TCG CCA GGG TT-3′ (F54L), 5′-TGC GGG GCG ATG CCG GCT CGC GTC GAG ATG GTC TGG AAC-3′ (F82A), 5′-GGG GCG ATG CCG TTA CGC GTC GAG ATG GT-3′ (F82L), 5′-AGA CGA TGC AAG CGT ACG CGA GCG AGG TCA ACC T-3′ (W116A), 5′-AGA CGA TGC AAG CAT ACT TTA GCG AGG TCA ACC T-3′ (W116F), and 5′-AGA CGA TGC AAG CAT ACT ATA GCG AGG TCA ACC T-3′ (W116Y) were synthesized and used as a primer for the respective mutagenesis; underlined nucleotides represent the ones changed by point mutations. The F54A, F54L, F82L, W116A, and W116F mutants were selected by digestions with *Ksp*I, *Eco*R47III, *Afl*III, *Spl*I, and T*th*lllII, respectively. The intended mutations were confirmed by determining the nucleotide sequence of the entire gene, using the dideoxynucleotide chain termination method (*25*). The mutated gene in pSK(−) was digested with *Eco*RI and *Hin*dIII to isolate the inserted DNA fragment and then subcloned into the same sites of pKK223-3 (Amersham Pharmacia Biotech). Each mutant enzyme as well as WT was produced in *E. coli* BL21DE3 (Novagen) and purified by deoxycholate affinity chromatography and Superose 12 gel filtration chromatography as described previously (*26*).

Activity Assay. The catalytic activity of the purified enzyme was determined spectrophotometrically using 5-AND or 5,10-EST as a substrate according to the previously described procedure (*26*). Various amounts of the substrate were added to the reaction buffer containing 34 mM potassium phosphate and 2.5 mM EDTA, pH 7.0, at 25 °C. The final concentrations of 5-AND were 12, 35, 58, 82, and 116 μM. The final concentration of methanol was 3.3 vol %. The reaction was stopped within 1 or 2 min after the initiation to obtain the initial reaction rate. The fraction of the overall conversion to the product was below 15%. The reaction was monitored by measuring the absorbance at 248 nm, using a spectrophotometer (Cary 3E). Kinetic data were analyzed with Lineweaver−Burk reciprocal plots to obtain k_{cat} and K_m.

Molecular Surface Area. Molecular surface areas were calculated from the atomic coordinates obtained by X-ray

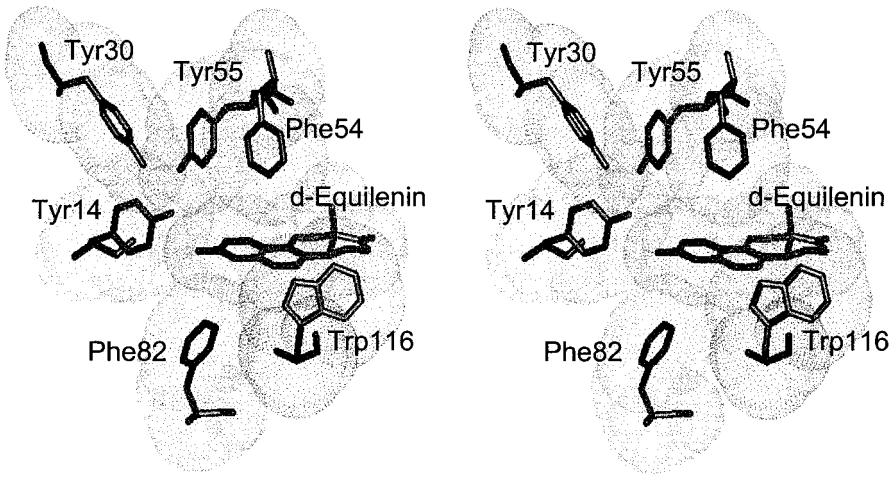

FIGURE 1: Stereoview of the aromatic residues in the active site of PI and their interactions with *d*-equilenin. The 150% van der Waals radius was drawn for each atom using the program Quanta, Version 2.0 (Molecular Simulations Inc.).

crystallography (*11*) using a program in Quanta, Version 2 (Molecular Simulations Inc.), based on the principle presented by Connolly (*27*).

Determination of K_D for Equilenin. Dissociation constant, K_D, for equilenin was determined by monitoring fluorescence quenching upon binding of equilenin to the enzyme. Fluorescence measurements were carried out at 25 °C with a spectrofluorometer (Shimadzu RF5000) in a buffer containing 10 mM potassium phosphate and 5% methanol at pH 7.0. Five microliters of the stock solution of equilenin was added to 3.0 mL of the buffer, giving the final concentration of 3 μM. Titrations were carried out by sequential additions of small aliquots (6−24 μL) of the enzyme solution with a total volume between 60 and 120 μL. Before and after the addition of enzyme, the emission spectrum of equilenin was scanned from 345 to 450 nm with an excitation wavelength at 335 nm. After the spectral change caused by the dilution had been corrected, the fluorescence of equilenin at the emission maximum (363−364 nm) for each enzyme concentration was used to calculate the K_D for equilenin by nonlinear least-squares fitting to eq 1 using a fitting program of Kaleidagraph version 2.6 (Abelbeck Software).

$$E_t = (F_0 - F)\{K_D/(F - F_\infty) + [\text{equilenin}]/(F_0 - F_\infty)\} \quad (1)$$

where E_t is the concentration of total enzyme in the solution, F is the fluorescence intensity, F_0 is the intensity in the absence of enzyme, and F_∞ is the intensity extrapolated to infinite enzyme concentration. A binding stoichiometry of 1 per subunit was assumed.

Determination of K_D for 19-Nortestosterone. The K_D for 19-nortestosterone was determined by analyzing ultraviolet absorption measurements. The measurements were carried out at 25 °C using a spectrophotometer (Cary 3E) in an 1.0 cm quartz cuvette with the total volume of 1 mL. The spectra from 320 to 220 nm were obtained in a solution containing 50 mM Tris-HCl and 100 mM sodium chloride, pH 7.0. The 19-nortestosterone was added to the enzyme successively from the stock solution of the steroid at 10 mM dissolved in 20% methanol. The absorbance change caused by the increased volume was corrected. Difference spectra were obtained by subtracting the spectra of total steroid and total enzyme from that of their mixture. The changes in absorption (ΔA) at the respective absorption maxima in the difference spectra were measured as a function of steroid concentration. Plots of ΔA with respect to total steroid concentration were fitted by eq 2 using the Kaleidagraph program.

$$\frac{\Delta A}{\Delta A_{max}} = \frac{K_D + E_t + S_t - \{(K_D + E_t + S_t)^2 - 4E_tS_t\}^{1/2}}{2E_t} \quad (2)$$

where K_D represents the dissociation constant, E_t the concentration of total enzyme, S_t the concentration of the total steroid, and ΔA_{max} the maximal change in absorption observed as S_t approaches infinity. A binding stoichiometry of 1 per subunit was assumed.

Crystallization and Structure Determination. Crystals of F82A were grown in a solution containing 1.0 M sodium acetate and 0.1 M ammonium acetate, pH 4.6, by the hanging drop method of vapor diffusion at 22 °C. The crystals belonged to the space group *C*2221 with unit cell dimensions of $a = 36.24$ Å, $b = 96.13$ Å, and $c = 74.30$ Å. Diffraction data were measured on a DIP2020 area detector with graphite-monochromated Cu Kα X-rays generated by a MacScience M18XHF rotating anode generator operated at 90 mA and 50 kV at room temperature. Data reduction, merging, and scaling were accomplished with the programs DENZO and SCALEPACK (*28*). The structure was determined by the molecular replacement program EPMR, using a highly refined monomeric model of the uninhibited PI. Further refinement was carried out by using the X-PLOR package (*29*). The final structure has been determined to 2.1 Å resolution. The root-mean-square deviations from ideal bond length and bond angle were 0.011 Å and 1.52°, respectively. The working R factor and R_{sym} were 20.9 and 7.2%, respectively.

RESULTS

Structural Analysis of the Interactions between the Aromatic Residues and Steroids. From the crystal structure of *P. putida* KSI in complex with *d*-equilenin (*11*), aromatic residues Tyr-14, Tyr-30, Phe-54, Tyr-55, Phe-82, and Trp-116 were identified to be closely located with respect to the steroid bound to the enzyme (Figure 1). Particularly, three aromatic residues, Phe-54, Phe-82, and Trp-116, facing the

Table 1: Distances (Å) and Angles between the Steroid Rings and the Aromatic Residues in the Active Site of PI[a]

	rings of *d*-equilenin				
	A	B	C	D	angle[b] (deg)
Phe-54	4.8 (C^{ζ}−C10) (6.0)	4.8 (C^{ζ}−C10) (6.0)	4.9 (C^{ζ}−C9) (6.5) 4.3 (C^{ζ}−C18)[c]	5.6 (C^{ζ}−C13) (7.0)	75
Phe-82	3.8 (C^{ζ}−C4) (5.5) 3.6 (C^{ζ}−O═C3)[d]	4.6 (C^{ζ}−C5) (6.5)	6.0 (C^{ζ}−C9) (8.0)	7.7 (C^{ζ}−C14) (9.0)	81
Trp-116, **I**	4.8 (N^{ϵ_1}−C5) (7.5)	3.6 (N^{ϵ_1}−C6) (6.0)	5.1 (N^{ϵ_1}−C8) (7.0)	4.8 (C^{ϵ_2}−C15) (7.5)	54
Trp-116, **II**	5.6 (C^{ϵ_2}−C5) (8.5)	4.1 (C^{ζ_2}−C7) (6.5)	5.0 (C^{ζ_2}−C8) (7.0)	4.1 (C^{η_2}−C15) (6.0)	

[a] The first row for each amino acid represents the nearest distance between the residue and the ring of equilenin with the corresponding atoms in parentheses. The number in parentheses represents the distance between the center of the aromatic ring of the amino acid and the ring of equilenin. [b] The angle between the plane of the aromatic residue and *d*-equilenin. [c] The distance between the C^{ζ} carbon of Phe-54 and the C18 carbon of the steroid. [d] The distance between the C^{ζ} carbon of Phe-82 and the C3 oxygen of the steroid. **I** and **II** represent the pentagonal and hexagonal rings of Trp-116, respectively. These data are based on the X-ray crystal structure of *P. putida* KSI (*11*).

steroid ring system seem to be crucial for binding steroids. The aromatic ring planes of Phe-54 and Phe-82 are almost perpendicular with the angles of 75° and 81° to the planes of the flat A and B rings in equilenin, respectively. Phe-54 approaches the β-face of the steroid, and its extensive interactions range from the A to D rings of the steroid with the A and B rings nearest to the residue. Phe-82 is positioned antarafacially with respect to Phe-54 in the enzyme−steroid complex and located more deeply in the active site cleft. Phe-82 mainly interacts with the A ring of the steroid. Trp-116-mediated interaction is also extensive with the B, C, D, and A rings in the order of distance from the residue. The indole ring plane of Trp-116 is oriented toward the bound steroid by an angle of about 54°. Distances between the centers of the aromatic ring in the residue and the steroid rings, nearest distances between them, and angles between the rings are listed in Table 1.

The molecular surface areas of the ring moieties of Phe-54, Phe-82, and Trp-116 were calculated to be 46, 11, and 52 Å^2, respectively, according to the previously described procedure (*27*) with a probe radius of 1.4 Å. These results suggest that the phenyl ring of Phe-82 is the most buried among the aromatic ring moieties while those of Phe-54 and Trp-116 are similarly exposed to solvent.

Preparation of Mutant Enzymes. To investigate whether Phe-54, Phe-82, and Trp-116 play any roles in performing high catalytic activity, they were individually mutated to generate such mutant enzymes as F54A, F54L, F82A, F82L, W116A, W116F, and W116Y. The mutant enzymes were produced in soluble forms similarly to WT and bound specifically to the deoxycholate affinity resin during the separation of each enzyme by affinity chromatography. The purified proteins were homogeneous as judged by SDS−PAGE analysis (data not shown). Each mutant enzyme exhibited a protein band of identical size on SDS−PAGE corresponding to a molecular mass of the 14 kDa monomer. The expression levels of the mutants were similar to that of WT with a yield of about 10 mg/200 mL culture.

Kinetic Properties. Kinetic parameters, k_{cat} and K_m, of WT and mutant enzymes toward two steroid substrates, 5-AND and 5,10-EST (Figure 2), were determined (Table 2). For 5-AND, k_{cat} was decreased by about 6-, 2-, and 8.4-fold for F54A, F54L, and F82L, respectively. This suggests that the phenylalanine side chain at position 54 is not crucial for catalysis and the leucine side chain at position 82 can substitute for the phenylalanine side chain, without significantly affecting the catalytic activity. However, k_{cat} was

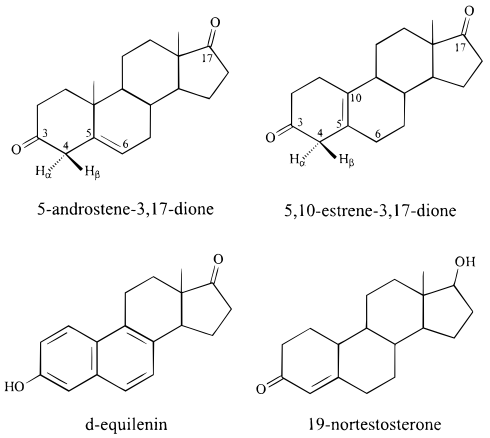

FIGURE 2: Structures of two reaction substrates, 5-androstene-3,17-dione and 5,10-estrene-3,17-dione, an analogue of the reaction intermediate, *d*-equilenin, and an analogue of the reaction product, 19-nortestosterone.

greatly decreased by ∼39-fold for F82A, suggesting that a space-filling hydrophobic side chain at position 82 is important for efficient catalysis. Among the tryptophan mutants, W116A had the most profound effect on the activity with an approximate 68-fold reduction in k_{cat} while W116F and W116Y decreased k_{cat} just by 4−5-fold. These results suggest that a bulky aromatic side chain is required at position 116 for the enzyme to perform efficient catalysis, and the polar hydroxyl group introduced newly in W116Y is tolerable for the catalysis. K_m increased for all but one mutant: F82A decreased K_m by ∼3-fold. The decrease in K_m by the F82A mutation suggests a possibility that the phenyl ring moiety of Phe-82 might give a negative effect on the stabilization of the enzyme−substrate complex. The K_m was increased by 3−4-fold for all the tryptophan mutants, implying that the indole ring moiety of Trp-116 might possibly be important for stabilizing the enzyme−substrate complex.

To investigate whether the mutations lead to alterations in the rate-limiting step for the reaction, 5,10-EST was used as a substrate and the ratio between k_{cat}'s toward 5-AND and 5,10-EST ($k_{cat}^{5-AND}/k_{cat}^{5,10-EST}$) was compared for the wild-type and mutant enzymes. Since 5,10-EST contains a double bond between C5 and C10, the ketonization step is very difficult to proceed compared with that for 5-AND (*30*, *31*). Concerning the rate-limiting step for TI, both enolization and ketonization are partially rate-limiting from kinetic isotope effects and disproportionation studies of the intermediate (*8*). If the ketonization becomes a rate-limiting step

Table 2: Kinetic Parameters of PI and Its Mutants toward 5-AND and 5,10-EST[a]

enzyme	substrate	k_{cat} (s^{-1})	K_m (μM)	k_{cat}/K_m ($M^{-1}\cdot s^{-1}$)	relative k_{cat}[b]	relative K_m[b]	$k_{cat}^{5-AND}/k_{cat}^{5,10-EST}$
WT	5-AND	21230 ± 810	49.9 ± 1.3	$(4.3 \pm 0.2) \times 10^8$	1.00	1.00	1910
	5,10-EST	11.1 ± 2.0	110 ± 15	$(1.0 \pm 0.3) \times 10^5$	1.00	1.00	
F54A	5-AND	3630 ± 110	57.9 ± 18.8	$(6.3 \pm 0.8) \times 10^7$	0.171	1.16	2200
	5,10-EST	1.7 ± 0.3	256 ± 30	$(6.6 \pm 2.0) \times 10^3$	0.153	2.33	
F54L	5-AND	8900 ± 1370	77.0 ± 9.9	$(1.2 \pm 0.2) \times 10^8$	0.419	1.54	2390
	5,10-EST	4.3 ± 1.5	98.2 ± 30.0	$(4.4 \pm 2.2) \times 10^4$	0.387	0.893	
F82A	5-AND	539 ± 22	14.9 ± 3.8	$(3.6 \pm 0.7) \times 10^7$	$10^{-1.6}$	0.299	2160
	5,10-EST	0.25 ± 0.10	32.8 ± 10.0	$(7.6 \pm 3.5) \times 10^3$	0.023	0.298	
F82L	5-AND	2540 ± 153	53.9 ± 9.0	$(4.7 \pm 0.3) \times 10^7$	0.120	1.08	339
	5,10-EST	7.5 ± 2.2	65.1 ± 10.1	$(1.2 \pm 0.4) \times 10^5$	0.676	1.30	
W116A	5-AND	311 ± 48.5	174 ± 19.3	$(1.8 \pm 0.2) \times 10^6$	0.015	3.48	>239[f]
	5,10-EST	<1.3[c]	>200[d]	—[e]	<0.117	>1.8	
W116F	5-AND	4760 ± 36	149 ± 20	$(3.2 \pm 0.2) \times 10^7$	0.224	2.99	>476[f]
	5,10-EST	<10[c]	>1000[d]	—[e]	<0.901	>9.1	
W116Y	5-AND	4420 ± 145	>200[d]	$<2.21 \times 10^7$	0.210	>4.00	>921[f]
	5,10-EST	<4.8[c]	>1000[d]	—[e]	<0.432	>9.1	

[a] The assays were performed at 25 °C in 34 mM potassium phosphate buffer containing 2.5 mM EDTA, pH 7.0, and 3.3% methanol. The values were obtained from three or five independent experiments. [b] Values relative to those of WT. [c] The upper limits were indicated due to the lack of precise measurements of k_{cat} for the tryptophan mutants. [d] The lower limits were indicated due to the lack of precise measurements of K_m for the tryptophan mutants. [e] The k_{cat}/K_m could not be determined due to the inaccuracy of k_{cat} and K_m for the tryptophan mutants. [f] The lower limit was estimated due to the inaccuracy of $k_{cat}^{5,10-EST}$.

for the reaction of the mutant enzymes, the k_{cat} toward 5,10-EST would be expected to significantly decrease, resulting in an increase of the ratio of $k_{cat}^{5-AND}/k_{cat}^{5,10-EST}$ compared with that of WT. Use of the 5,10-EST as a substrate resulted in a decrease of k_{cat} giving the ratio of $k_{cat}^{5-AND}/k_{cat}^{5,10-EST}$ to be ca. 2000 for WT. For F54A, F54L, F82A, and W116Y, the $k_{cat}^{5-AND}/k_{cat}^{5,10-EST}$ was similar to that for WT, while the $k_{cat}^{5-AND}/k_{cat}^{5,10-EST}$ for F82L, W116A, and W116F was decreased by 2−8-fold compared to that for WT, implying that the ketonization might not be the rate-limiting step for these mutants. The K_m value was increased by ~2.2-fold for WT and F82A, by ~4.4-fold for F54A, and marginally for F54L. The tryptophan mutants exhibited high values of K_m for 5,10-EST, suggesting that the indole ring of Trp-116 might be important for the interaction with 5,10-EST.

Effect of Mutations on Equilenin Binding. The K_D for *d*-equilenin (Figure 2) was determined by analyzing the fluorescence emission spectra of equilenin while varying the enzyme concentration. The excitation wavelength of 335 nm was used to monitor the binding of equilenin without any disturbance originating from the quenching of the intrinsic fluorescence of the protein upon its binding of equilenin. The representative spectra for WT are shown in Figure 3. The spectra for other mutants were similar to that of WT. Equilenin exhibited the maximum emission peak at 363−364 nm when excited with a wavelength at 335 nm. Addition of the enzyme caused a marked decrease in the intensity of this peak due to the quenching of the fluorescence by the protein, but no shift of λ_{max} was observed.

Fluorescence intensity at 363 nm monitored in the absence or presence of the enzyme at various concentrations was analyzed as a function of the concentration of the added enzyme (Figure 4). The K_D value was obtained from the observed fluorescences according to the relationship given by eq 1. The experimental data were nicely fitted to eq 1 with the correlation coefficient, *R*, higher than 0.999. The K_D value was determined to be 1.9 ± 0.2 μM for WT (Table 3). Relative to WT, the K_D was largely increased by about 8.3-, 19.2-, 13.2-, and 12.6-fold for F54A, F82A, F82L, and W116Y, respectively, and marginally increased by about 1.3-, 1.9-, and 3.1-fold for F54L, W116A and W116F, respectively. A marked increase in the K_D of *d*-equilenin for F54A as compared with that for F54L indicates that the space-filling hydrophobic side chain at position 54 might be important for binding the reaction intermediate. The large decreases in the affinity for both F82A and F82L suggest that the phenylalanine side chain at position 82 might be important for the enzyme to efficiently bind a reaction intermediate. The affinity toward equilenin was also largely decreased for W116Y, indicating that the tyrosine side chain at position 116 gives a negative effect on binding equilenin.

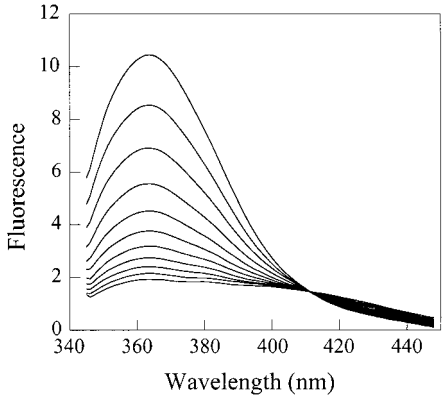

FIGURE 3: Fluorescence emission spectra of equilenin observed at different concentrations of added enzyme in the buffer containing 10 mM phosphate and 5% methanol, pH 7.2, for the wild-type PI. The equilenin concentration was 3 μM. Enzyme concentrations were increased by 1 μM from 0 to 10 μM in the order of decreasing fluorescence intensity. The ordinate represents the relative fluorescence intensity.

Effect of Mutations on 19-Nortestosterone Binding. The K_D for 19-nortestosterone (Figure 2), an analogue of the reaction product, was determined by analyzing the changes in UV absorption spectra upon binding 19-nortestosterone to the enzyme. Upon complexation with 19-nortestosterone, the WT, F54A, F54L, and W116Y enzymes exhibited maxima in the difference spectrum at 269−272 nm. The UV absorption spectrum of 19-nortestosterone also changed upon its binding to the enzyme (Figure 5); λ_{max} of the absorption spectrum was shifted from 247 to 257 nm for WT and

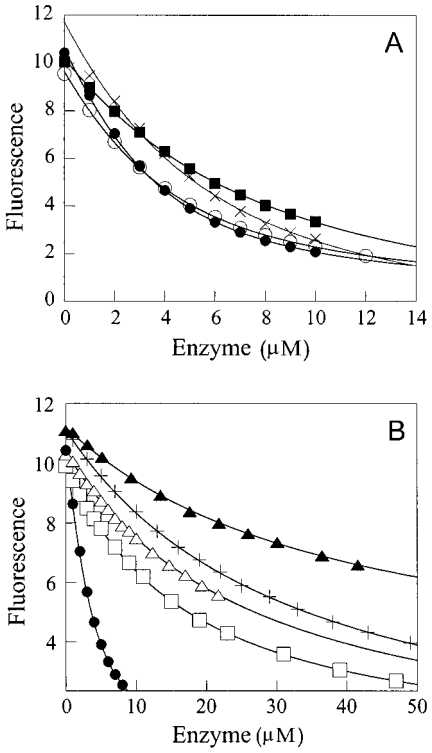

FIGURE 4: Changes of fluorescence emission of equilenin at 363 nm by varying the enzyme concentration for WT (●), F54L (○), W116A (×), and W116F (■) in (A) and for WT (●), F54A (□), F82A (▲), F82L (+), and W116Y (△) in (B). The excitation wavelength was 335 nm. The curves were obtained by fitting the data points to eq 1. The ordinate represents the relative fluorescence intensity.

Table 3: Dissociation Constants (K_D) on Binding of *d*-Equilenin and 19-Nortestosterone to PI Wild Type and Its Mutants

enzyme	K_D (μM)	
	d-equilenin[a]	19-nortestosterone[b]
wild type	1.9 ± 0.2	7.3 ± 1.6 (272)[c]
F54A	15.7 ± 0.3	3.6 ± 0.5 (270)
F54L	2.4 ± 0.1	0.5 ± 0.2 (270)
F82A	36.4 ± 1.0	>30[d]
F82L	25.0 ± 3.0	8.1 ± 1.0 (269)
W116A	3.6 ± 0.7	2.3 ± 0.7 (290)
W116F	5.8 ± 0.2	4.8 ± 0.4 (289)
W116Y	23.9 ± 1.1	3.3 ± 0.8 (272)

[a] K_D for *d*-equilenin was obtained in the buffer containing 10 mM phosphate and 5% methanol, pH 7.22. [b] K_D for 19-nortestosterone was obtained in the buffer containing 50 mM Tris-HCl, 100 mM NaCl, pH 7.0, and methanol below 1% by volume. [c] The values in parentheses represent the wavelength (nm) exhibiting the maximum of the difference spectrum which was obtained by subtracting the spectra of the total enzyme and total nortestosterone from that of the enzyme−nortestosterone complex. [d] The lower limit was indicated due to the very low level of the difference spectrum even with 19-nortestosterone in a 5-fold molar excess amount relative to the enzyme. The values were obtained from three or five independent experiments.

W116Y and to 260, 262, and 253 nm for F54L, F54A, and F82L, respectively. These spectral changes are considered to result from a short strong hydrogen bond to O3 of the steroid (*32*, *33*). On the other hand, W116A and W116F exhibited the maximum of the difference spectrum at 290 and 289 nm, respectively, and λ_{max} of the absorption spectrum of 19-nortestosterone bound to these enzymes was almost similar to that of the free steroid. This result suggests that O3 of 19-nortestosterone might hardly make a hydrogen bond

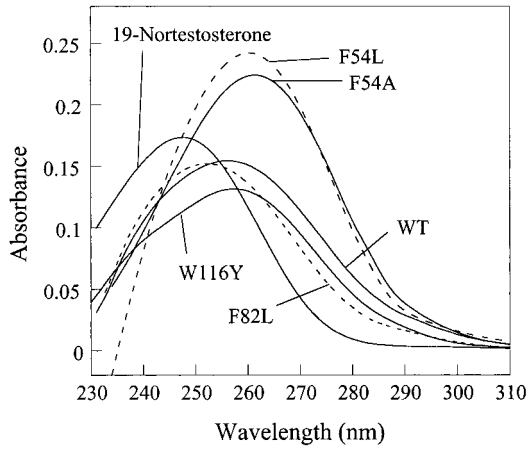

FIGURE 5: Effects of the binding of 19-nortestosterone to an enzyme on the ultraviolet absorption spectrum of the steroid. The spectrum of free 19-nortestosterone at 9.5 μM in the buffer as well as those of 19-nortestosterone bound to WT, F54A, F54L, F82L, and W116Y are represented, respectively. The spectra of both total enzyme and free steroid were subtracted from the spectrum of the steroid−enzyme mixture. The total concentration of 19-nortestosterone was 15 μM in the buffer containing 50 mM Tris-HCl and 100 mM sodium chloride, pH 7.0. The concentrations of 19-nortestosterone bound to the enzymes were 9.5, 11.3. 14.4, 10.3, and 7.11 μM for WT, F54A, F54L, F82L, and W116Y, respectively. The methanol concentration was 0.75 vol %.

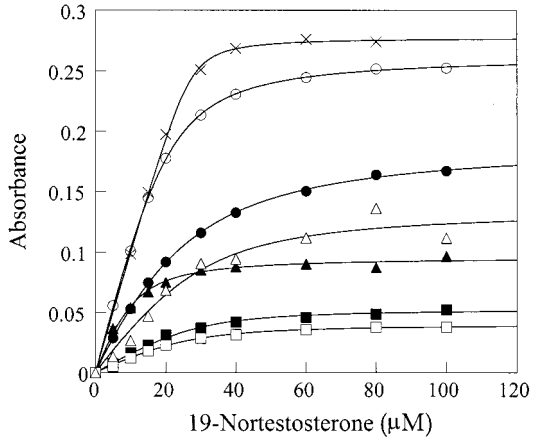

FIGURE 6: Ultraviolet spectral titrations for assessing the interaction of enzymes with 19-nortestosterone. For each enzyme, a difference spectrum was obtained by subtracting the spectra originated from the total steroid and total enzyme from that of their mixture. The absorption maximum of the difference spectrum for WT (●), F54A (○), F54L (×), F82L (△), W116A (■), W116F (□), and W116Y (▲) was analyzed as a function of total steroid concentration. The curves were obtained by fitting the data to eq 2. The buffer used was 50 mM Tris-HCl and 100 mM NaCl, pH 7.0, and the final concentration of methanol was 2 vol %.

with Tyr-14 or Asp-99 upon binding to W116A and W116F, which might be explained by the nonproductive orientation of the bound steroid (*14*, *21*, *34*). Thus, the bulky indole ring moiety at position 116 appears to be important for orientation of the bound steroid to make a hydrogen bond between Tyr-14 Oη or Asp-99 Oδ2 and O3 of the steroid.

From the spectral titration with changing the steroid concentration, K_D of 19-nortestosterone was obtained for each enzyme according to the relationship given by eq 2. Such spectral titrations for WT and the seven mutant enzymes are shown in Figure 6. WT was found to bind 19-nortestosterone with a K_D of 7.3 ± 1.6 μM (Table 3). The K_D was decreased

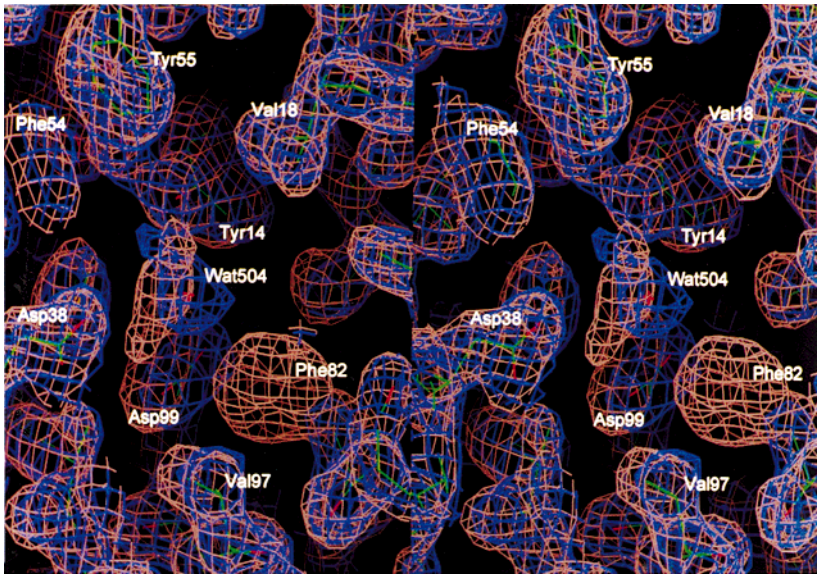

FIGURE 7: Stereo diagram of a section of the electron density map ($2F_0 - F_c$ coefficients, contoured at 1.0σ) of the active site for WT (brown) calculated with the final model of WT previously obtained (*11*) and for F82A (blue) calculated after the refinement of the F82A structure. The final protein model of the mutant enzyme is shown as a stick figure. This figure was prepared using the program Chain (*35*).

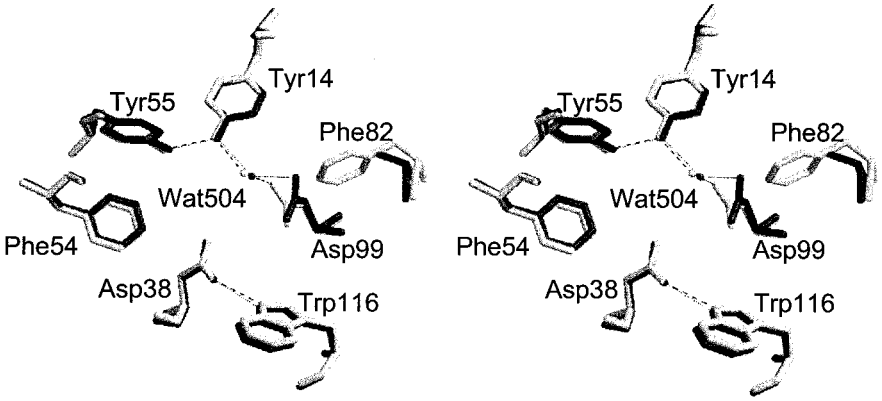

FIGURE 8: Stereoview of active site residues of WT and F82A after the superposition of the backbone atoms of all residues. The amino acids of WT are shown in gray, and those of F82A are shown in black. The possible hydrogen bonds are indicated by dashed lines. The root-mean-square deviations for the main-chain atoms and for all the atoms in the displayed residues are 0.15 and 0.27 Å, respectively. The program Quanta, Version 2.0 (Molecular Simulations Inc.), was used for the superposition. The program Molscript (*36*) was used for drawing the figure.

by about 2- and 15-fold for F54A and F54L, respectively, relative to WT. The higher affinity of F54L for 19-nortestosterone reveals a possibility that the mutant enzyme can bind the reaction product more tightly than WT. For W116A, K_D was decreased by about 3-fold, implying that the bulky aromatic ring at position 116 contributes to destabilization of the enzyme−product complex. The F82L mutant exhibited the similar level of K_D as WT while the W116F and W116Y mutations decreased K_D by about 1.5- and 2-fold, respectively. The F82A mutant exhibited a very low level of the difference spectrum even with 19-nortestosterone in 5-fold molar excess amount relative to the enzyme. This may imply that the F82A mutant might bind the product very weakly.

Local Structural Perturbation by the F82A Mutation. To explain the observed changes in the binding affinity of F82A toward the steroid species on the structural basis, the crystal structure of F82A was determined at 2.1 Å resolution with accumulated completeness 95.8% (outer shell, 2.19∼2.10, 91.2%) by molecular replacement. Even if the overall structure of F82A does not show any significant difference compared with that of WT, a closer examination of the F82A structure around the site of the mutation reveals that Asp-99 Oδ2 and Wat-504 O are displaced about 1.39 and 0.68 Å, respectively, toward the cavity newly generated by the mutation (Figures 7 and 8). Other ordered water molecules are not detected in the cavity. As shown by the superposition of the active site residues, the hydrogen bond distance between Asp-99 Oδ2 and Wat-504 O increases from 2.91 ± 0.25 to 3.24 ± 0.26 Å, and the distance between Tyr14 Oη and Asp-99 Oδ2 also increases from 3.96 ± 0.25 to 4.53 ± 0.26 Å with a standard deviation for each distance evaluated on the basis of the estimation by Luzzati plots (*37*).

DISCUSSION

The analysis of kinetic and binding constants has allowed us to estimate the effects of the mutations of the aromatic residues Phe-54, Phe-82, and Trp-116 at the active site of PI on the stabilization of substrate, intermediate, product, and transition state bound to the enzyme. The affinities of the reaction intermediate and the product for KSI were deduced from the binding affinities of their analogues. The

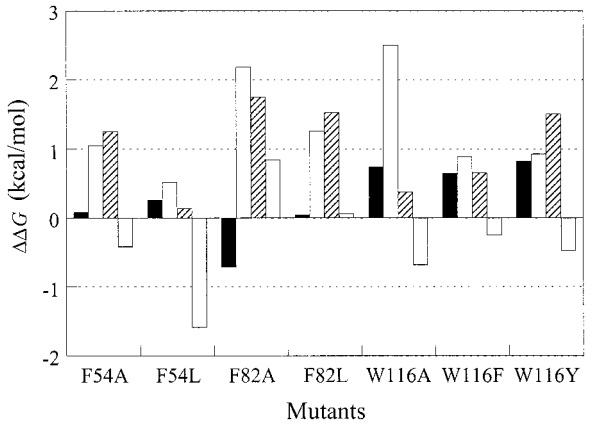

FIGURE 9: Differences in free energy changes ($\Delta\Delta G$ or $\Delta\Delta G^{\ddagger}$) associated with K_m (closed bar), k_{cat} (open bar), and K_D values toward *d*-equilenin (hatched bar) and 19-nortestosterone (shaded bar) for the mutant enzymes relative to the wild-type enzyme. Calculations were performed according to eq 3 using the values listed in Tables 2 and 3.

effect of mutations on the stabilization of the transition state was estimated by comparing the ratio of k_{cat} or k_{cat}/K_m between WT and mutant enzymes (*38*). The effect of mutation on the substrate binding is somewhat complicated to assess. Even though K_m is not an accurate measure of substrate binding in this enzyme, K_m would be expected to approximately reflect K_s, especially for the reaction in which chemical steps are rate-limiting. For the wild-type enzyme of TI, K_m was taken to be a good estimate of K_s (*15*, *21*).

The energetic perturbation affected by the respective mutations relative to the wild-type enzyme was evaluated on the basis of the difference in the free energy change, which was calculated using the equations:

$$\Delta\Delta G_m = -RT \ln(K_m^{WT}/K_m^{mutant}) \quad (3a)$$

$$\Delta\Delta G^{\ddagger} = -RT \ln(k_{cat}^{mutant}/k_{cat}^{WT}) \quad (3b)$$

$$\Delta\Delta G_D = -RT \ln(K_D^{WT}/K_D^{mutant}) \quad (3c)$$

where $\Delta\Delta G_m$, $\Delta\Delta G^{\ddagger}$, and $\Delta\Delta G_D$ represent the differences in free energy changes associated with K_m, k_{cat}, and K_D, respectively. The calculated mutational effects are represented graphically in Figure 9. A negative value of $\Delta\Delta G$ indicates that the mutant enzyme has a more favorable equilibrium for binding or an increased rate constant.

Phenylalanine 54. The replacement of Phe-54 by a small nonaromatic amino acid, alanine, results in a moderate reduction in the activity (Table 2 and Figure 9). The more pronounced decrease in activity as a result of the F54A mutation as compared with the F54L mutation is probably a result of the loss of hydrophobic interactions mediated by the bulky nonpolar side chain. Interestingly, the binding affinity for 19-nortestosterone, among the enzymes, is highest for F54L (Table 3). This result might be explained by the optimization of the structural complementarity between the enzyme and the steroid when the leucine side chain, having a smaller mean volume than the phenylalanine side chain, occupies position 54. The difference in affinity toward equilenin and 19-nortestosterone for WT, F54A, and F54L suggests that the phenyl ring moiety of Phe-54 might be favorable for binding the reaction intermediate but unfavorable for binding the product. The binding interactions mediated by Phe-54 are estimated to contribute 0.5−1 kcal/mol to catalysis on the basis of the decrease in k_{cat} by the mutations (Figure 9).

Phenylalanine 82. Interestingly, all of the mutant enzymes except F82A display an increased K_m, whereas only the F82A mutation decreases K_m (Table 2). The decrease in K_m might result from either an increase in affinity for the substrate or a decrease in the rate constant for the conversion of the substrate to the reaction intermediate. The stabilization of the enzyme−substrate complex relative to the transition state would lead to a reduction in the reaction rate since the stabilization may contribute to a higher activation energy barrier. However, the 39-fold reduction in k_{cat}, which corresponds to ca. 2 kcal/mol in energy difference, does not seem to be totally explained by the relative stabilization of the enzyme−substrate complex which could be roughly approximated to be just ca. 0.8 kcal/mol from the K_m values according to the equation, $RT \ln(K_m^{WT}/K_m^{F82A})$. The additional energy of about 1.2 kcal/mol might have originated from the destabilization of the transition state of the rate-limiting step. The ratio of k_{cat}/K_m between WT and F82A gives ca. 1.4 kcal/mol as the energy for the destabilization of the transition state caused by the F82A mutation. Therefore, the phenyl ring moiety of Phe-82 is considered to be important for the stabilization of the transition state for the rate-limiting step. Meanwhile, the large decrease in the binding affinity toward equilenin for F82A and F82L (Table 3 and Figure 9) implies that the phenyl ring of Phe-82 might also be important for interactions with the reaction intermediate. It is noticeable that the F82A mutation is unique among the mutations in that it increases K_D for 19-nortestosterone significantly relative to WT. This result, together with the finding that the F82L mutation does not significantly change the K_D, suggests that a bulky hydrophobic side chain at position 82 might be necessary to efficiently bind the product.

In addition to providing the binding energy for catalysis, Phe-82 plays a role in maintaining the active site geometry as revealed by the crystal structure of F82A. The crystal structure reveals a local structural perturbation of the active site geometry leading to the positional shift of Asp-99 and Wat-504 (Figures 7 and 8). This positional displacement leads to the alteration of the geometry of the hydrogen bonds; in F82A, the hydrogen bond between Asp-99 Oδ2 and Wat-504 O is an average of 0.33 ± 0.25 Å longer and the Asp-99 Oδ2 is displaced about 0.57 ± 0.25 Å away from Tyr-14 Oη. Such a change in the active site geometry might contribute differentially to the stabilization of the reaction species of the steroids. The steroid species of substrate, intermediate, and product are predicted to be different in their ring structures accompanied by the change in the orientation of the O3 (Figure 10). The O3 of the substrate would be expected to be positioned more optimally between Tyr-14 Oη and Asp-99 Oδ2 in F82A than in WT, which probably results in the higher stabilization of the substrate bound to F82A. In the cases of the mutations of Phe-54 and Trp-116, the structural perturbation may not be so significant, even if it occurs, since these residues are highly exposed to solvent compared with Phe-82 which is located deeply in the active site pocket.

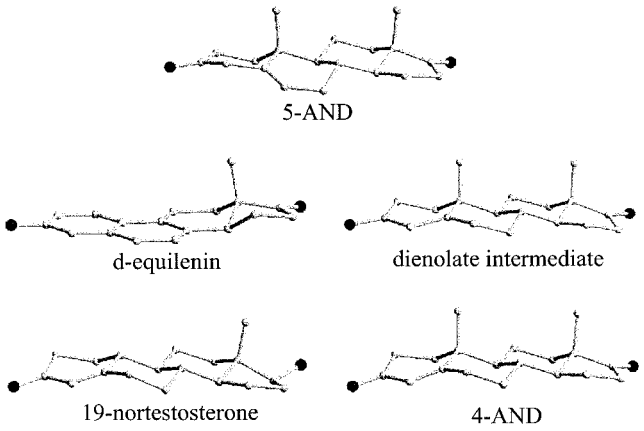

FIGURE 10: Ball-and-stick model of the crystal structures of steroids of 5-AND (*39*), *d*-equilenin (*11*), 19-nortestosterone (*40*), and 4-AND (*41*) and of the predicted structure of the dienolate intermediate which was obtained from an energy minimization using the program CHARMM in Quanta, Version 2.0. The oxygen atoms are indicated in black.

Trptophan 116. The importance of an aromatic residue for position 116 is underscored by the 68-fold drop in k_{cat} upon mutating Trp-116 to alanine (Table 2). The smaller decrease in k_{cat}, observed as a result of the W116F and W116Y mutations, is probably due in part to the bulky aromatic nature of the side chains. The 3- or 4-fold increase in K_m for all the tryptophan mutants suggests that the indole ring of Trp-116 might be favorable for binding the substrate (Table 2 and Figure 9). The drastic decrease in the affinity toward equilenin for W116Y is probably a result of protrusion of the tyrosine side chain into the steroid binding pocket, thus introducing an unfavorable steric interaction with the bound equilenin. Even if marginal, the 1.5−3-fold decrease in K_D of 19-nortestosterone for the tryptophan mutants implies that the bulky tryptophan side chain at position 116 might be unfavorable for product binding. Such a differential stabilization for the steroid species might be related to the conformational change of the steroid species (Figure 10). The structural change of the B ring during catalysis might affect the interaction between the steroid and the indole ring of Trp-116, resulting in the differential binding affinity toward the steroid species. Meanwhile, the putative nonproductive binding of 19-nortestosterone to the W116A and W116F enzymes implies that the tryptophan residue might be important for the orientation of the bound steroid to position the O3 of the steroid precisely within the hydrogen bond distance from Tyr14 Oη.

In addition to the contribution of Trp-116 to the steroid binding through which it may interact with the bound substrate and inhibitors, the examination of the crystal structure of PI reveals that Trp-116 is involved in a hydrogen bond with the side-chain carboxyl oxygen of Asp-38 (Figure 8). The distance between Asp-38 Oδ1 and Trp-116 Nϵ1 is about 2.91 ± 0.26 Å. Even though the hydrogen bond does not seem to be significant for catalysis as reflected in the marginal effects of the W116F and W116Y mutations on k_{cat}, the elimination of this hydrogen bond might possibly affect the catalytic role of Asp-38 as a general base. The binding energy provided by Trp-116 is estimated to contribute 1−2.5 kcal/mol to catalysis on the basis of the decrease in k_{cat} by the mutations (Figure 9).

Although the affinities for the analogues of the reaction intermediate and product might be different from those for the authentic reaction species in the enzymatic reaction, our studies demonstrate that the aromatic residues contribute differentially to the stabilization of the steroid species bound to the enzyme. The structural analysis of F82A leads us to speculate that the other mutations might exert their mutational effects on steroid binding by perturbing the hydrogen-bonding interactions between the catalytic side chains and O3 of the steroid. The determination of the crystal structure of the mutant enzymes, particularly in the presence of an intermediate analogue such as equilenin, will contribute to better understanding of the effects of the mutations on catalysis and the binding affinity for the steroid molecules.

ACKNOWLEDGMENT

We thank Byeung Doo Song and Suhng Wook Kim for helpful discussion and comments, Nam Chul Ha for assistance with graphic works, and Ja Heon Kim for help with searching the crystal structures of the steroid molecules. We appreciate very much the help of Alice Dana Walker in POSTECH for improving the English of the manuscript.

REFERENCES

1. Batzold, F. H., Benson, A. M., Covey, D. F., Robinson, C. H., and Talalay, P. (1976) *Adv. Enzyme Regul. 14*, 243−267.
2. Schwab, J. M., and Henderson, B. S. (1990) *Chem. Rev. 90*, 1203−1245.
3. Xue, L., Talalay, P., and Mildvan, A. S. (1990) *Biochemistry 29*, 7491−7500.
4. Kuliopulos, A., Mullen, G. P., Xue, L., amd Mildvan, A. S. (1991) *Biochemistry 30*, 3169−3178.
5. Wang, S.-F., Kawahara, F. S., and Talalay, P. (1963) *J. Biol. Chem. 238*, 576−585.
6. Pollack, R. M., Mack, J. P. G., and Eldin, S. (1987) *J. Am. Chem. Soc. 109*, 5048−5050.
7. Xue, L., Kuliopulos, A., Mildvan, A. S., and Talalay, P. (1991) *Biochemistry 30*, 4991−4997.
8. Hawkinson, D. C., Eames, T. C., and Pollack, R. M. (1991) *Biochemistry 30*, 10849−10858.
9. Hawkinson, D. C., Pollack, R. M., and Ambulos, N. P., Jr. (1994) *Biochemistry 33*, 12172−12183.
10. Kuliopulos, A., Talalay, P., and Mildvan, A. S. (1990) *Biochemistry 29*, 10271−10280.
11. Kim, S. W., Cha, S.-S., Cho, H.-S., Kim, J.-S., Ha, N.-C., Cho, M.-J., Joo, S., Kim, K.-K., Choi, K. Y., and Oh, B.-H. (1997) *Biochemistry 36*, 14030−14036.
12. Cho, H.-S., Choi, G., Choi, K. Y., and Oh, B.-H. (1998) *Biochemistry 37*, 8325−8330.
13. Wu, Z. R., Ebrahimian, S., Zawrotny, M. E., Thornburg, L. D., Perez-Alvarado, G. C., Brothers, P., Pollack, R. M., and Summers, M. F. (1997) *Science 276*, 415−418.
14. Massiah, M. A., Abeygunawardana, C., Gittis, A. G., and Mildvan, A. S. (1998) *Biochemistry 37*, 14701−14712.
15. Xue, L., Talalay, P., and Mildvan, A. S. (1991) *Biochemistry 30*, 10858−10865.
16. Kim, S. W., Joo, S., Choi, G., Cho, H.-S., Oh, B.-H., and Choi, K. Y. (1997) *J. Bacteriol. 179*, 7742−7747.
17. Gerlt, J. A., and Gassman, P. G. (1993) *J. Am. Chem. Soc. 115*, 11552−11568.
18. Zhao, Q., Abeygunawardana, C., Talalay, P., and Milvan, A. S. (1996) *Proc. Natl. Acad. Sci. U.S.A. 93*, 8220−8224.
19. Zhao, Q., Abeygunawardana, C., and Mildvan, A. S. (1997) *Biochemistry 36*, 3458−3472.
20. Zhao, Q., Abeygunawardana, C., Gittis, A. G., and Mildvan, A. S. (1997) *Biochemistry 36*, 14616−14626.

21. Brothers, P. N., Blotny, G., Qi, L., and Pollack, R. M. (1995) *Biochemistry 34*, 15453−15458.
22. Qi, L., and Pollack, R. M. (1998) *Biochemistry 37*, 6760−6766.
23. Kunkel, T. A. (1985) *Proc. Natl. Acad. Sci. U.S.A. 82*, 488−492.
24. Kim, S. W., and Choi, K. Y. (1995) *J. Bacteriol. 177*, 2602−2605.
25. Sanger, F., Nicklen, S., and Coulson, A. R. (1977) *Proc. Natl. Acad. Sci. U.S.A. 74*, 5463−5467.
26. Kim, S. W., and Choi, K. Y. (1994) *J. Bacteriol. 176*, 6672−6676.
27. Connolly, M. L. (1993) *J. Mol. Graphics 11*, 139−141.
28. Otwinoski, Z., and Minor, W. (1997) *Methods Enzymol. 276*, 307−326.
29. Brunger, A. T. (1992) *X-PLOR Version 3.0*, Yale University Press, New Haven, CT.
30. Holman, C., and Benisek, W. (1994) *Biochemistry 33*, 2672−2681.
31. Holman, C., and Benisek, W. (1995) *Biochemistry 34*, 14245−14253.
32. Kuliopulos, A., Mildvan, A. S., Shortle, D., and Talalay, P. (1989) *Biochemistry 28*, 149−159.
33. Hawkinson, D. C., and Pollack, R. M. (1993) *Biochemistry 32*, 694−698.
34. Bevins, C. L., Pollack, R. M., Kayser, R. L., and Bounds, P. L. (1986) *Biochemistry 25*, 5159−5164.
35. Sack, J. S. (1988) *J. Mol. Graphics 6*, 224−225.
36. Kraulis, P. J. (1991) *J. Appl. Crystallogr. 24*, 946−950.
37. Luzzati, P. V. (1952) *Acta Crystallogr. 5*, 802−810.
38. Fersht, A. (1985) in *Enzyme Structure and Mechanism*, 2nd ed., pp 294−346, W. H. Freeman and Co., New York.
39. Carrell, H. L., Glusker, J. P., Covey, D. F., Batzold, F. H., and Robinson, C. H. (1978) *J. Am. Chem. Soc. 100*, 4282−4289.
40. Bhadbhade, M. M., and Venkatesan, K. (1984) *Acta Crystallogr., Sect. C (Crystal Struct. Commun.) 40*, 1905.
41. Busetta, B., Comberton, G., Courseille, C., and Hospital, M. (1987) *Crystal Struct. Commun. 1*, 129.

BI991040M